

1

Introduction

It is appropriate to begin this introduction with a thoughtful reminder by Sir Geoffrey Ingram Taylor (1974): “Though the fundamental laws of the mechanics of the simplest fluids, which possess Newtonian viscosity, are known and understood, to apply them to give a complete description of any industrially significant process is often far beyond our power.” This is particularly true for oil-hungry mankind’s desire for hydrocarbons, with pollution as a bonus. The principal difficulties stem from the problems associated with the determination of the state of the sea, the three-dimensional and random nature of the ocean–structure interaction, quantification of the forces exerted on structures, and the lack of a fluid-mechanically satisfying closure model for turbulence. The past hundred years have shown that “almost-randomness” is the law of the physics of turbulence. One can quantify the consequences of turbulence and probe into its behavior for a given event only through approximate models and physical and numerical experiments (provided that the wideband of relevant scales is fully resolved). Even if the direct numerical simulations (DNSs) at Reynolds numbers as high as 10^7 were possible in the centuries to come, the large parameter space in any application precludes a purely numerical solution.

The past four decades have seen an explosion of interest in the broad subject of ocean hydrodynamics. This interest led to an improved and more realistic understanding of the physical characteristics of some time-dependent flows about bluff bodies and their mathematical formulation and experimental exploration. On the one hand, attention has been focused on controlled laboratory experiments, which allow for the understanding of the separate effects of the governing and influencing parameters, and, on the other hand, on mathematical and numerical methods, which allow for the nearly exact solution of some wave-loading situations (large bodies, whose volumes are as large as 10 times that of the great pyramid of Khufu). For many practically significant fluid–structure interactions involving flow separation, vortex motion, turbulence, dynamic response, and structural and fluid-dynamical

damping, however, direct observations and measurements are continuing to provide the needed information, whereas theory has not yet played an important role.

The hydrodynamic loading situations that are well understood are those that do not involve flow separation. Thus they are amenable to nearly exact analytical treatment. These concern primarily the determination of the fluid forces on large objects in the diffraction regime where the characteristic dimension of the body relative to the wavelength is larger than about 0.2. The use of various numerical techniques is sufficient to predict accurately the forces and moments acting on the body, provided that the viscous effects and the effects of separation for bodies with sharp edges are ignored as secondary.

The understanding of the fluid–structure interactions that involve extensive separation and dependence on numerous parameters, such as the Reynolds number and the Keulegan–Carpenter number $K = 2\pi(A/D)$, a parameter that does not depend on time (it is a simple length ratio). There are several reasons for this. First, although the physical laws governing motion (the Navier–Stokes equations) are well known, valid approximations necessary for numerical and physical model studies are still unknown. Even the unidirectional steady flow about a bluff body remains theoretically unresolved. Fage and Johansen’s (1928) pioneering work and Gerrard’s (1965) vortex-formation model, followed by a large number of important experiments, have provided extremely useful insights into the mechanism of vortex shedding. It became clear that a two-dimensional ambient flow about a two-dimensional body does not give rise to a two-dimensional wake, and only a fraction (about 60% for a circular cylinder) of the original circulation survives the vortex formation.

Offshore technology has experienced a remarkable growth since the 1940s, when offshore drilling platforms were first used in the Gulf of Mexico. At the present time, a wide variety of offshore structures are being used, even under severe environmental conditions. These are predominantly related to oil and gas recovery, but they are also used in other applications such as harbor engineering and ocean energy extraction. Difficulties in design and construction are considerable, particularly as structures are being located at ever-increasing depths and are subjected to extremely hostile environmental conditions. The discovery of major oil reserves in the North Sea has accelerated such advances, with fixed platforms in the North Sea, now located in water depths up to about 185 m and designed to withstand waves as high as 30 m. In more recent years the depths to be reached for more hydrocarbon resources have increased to 1600 m or more. In fact, the depths reached during the past 55 years increased as $h \approx (1/540)N^{3.5}$,

where h is the depth and N is the number of years, starting with $N = 0$ in 1949.

The potential of major catastrophic failures, in terms of both human safety and economic loss, underlines the critical importance of efficient and reliable design. In January 1961, the collapse of Texas Tower No. 4 off the New Jersey coast involved the loss of 28 lives. In March 1980, the structural failure and capsizing of the mobile rig *Alexander Keilland* in the Ekofisk field in the North Sea involved the loss of over 100 lives. The *Piper Alpha* oil and gas platform caught fire in 1988, leading to the loss of 167 lives. The *Petrobras* (a floating production system) sank in the Campos Basin in 2001 and cost 10 lives.

1.1 Classes of offshore structures

It is appropriate at the outset to provide some perspective to what follows by classifying briefly the wide variety of offshore structures that are in current use or that have been seriously proposed. The major offshore structures used in the various stages of oil recovery include both mobile and fixed drilling platforms, as well as a variety of supply, work, and support vessels.

The various offshore structures currently in use have been described in detail in the trade and technical literature. Mention is made of Bruun (1976), who summarized the offshore rigs used in the North Sea, and Watt (1978), who reviewed the design and analysis requirements of fixed offshore structures used in the oil industry. Ships and moored shiplike marine vessels are also used extensively, but they are treated within the field of naval architecture and are not of primary consideration in this book.

In earlier years the development and production activities at an offshore site were primarily carried out with fixed platforms. The jacket or template structures, and extensions to them, were the most common platforms in use. A jacket platform comprises a space frame structure, with piles driven through its legs. An extension to this concept includes the space frame structures that employ skirt piles or pile clusters. Some platforms contain enlarged legs to provide for self-buoyancy during installation. Jacket platforms are located throughout the world, including the North Sea, where they may be exposed to waves with heights approaching 100 ft.

Figure 1.1 shows numerous structures with a variety of names [fixed platforms: gravity-based structures (GBSs) and the jacket]. These are followed by guyed and compliant towers. Under the general title of floating structures, there are tension leg platforms (TLPs), SPAR-buoys, and floating production systems (FPSs). The largest platform until 1980 was one installed in the Cognac field off the Louisiana coast in a water depth of just over

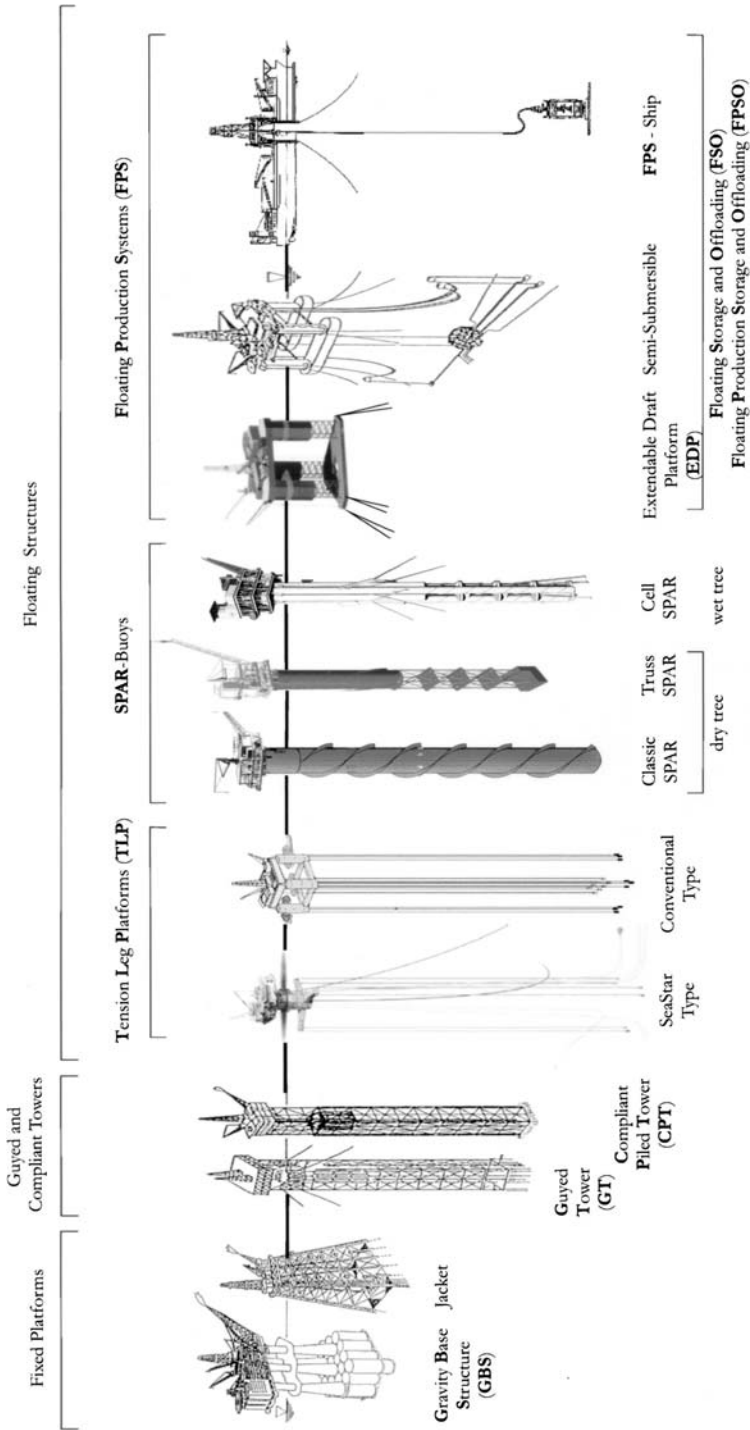


Figure 1.1. Representative offshore platforms (after Günther F. Claus 2007).

300 m. This platform contained 60 000 metric tons of steel and was fabricated in three sections, which were joined under water on site.

Gravity platforms depend on excessive weight, rather than on piles, for their stability. They are thus suited to sites with overconsolidated soils and have been used primarily in the North Sea. The most usual gravity platforms comprise a large base, which has the capacity for significant oil storage. In addition to their being located in depths of several hundred feet, gravity platforms are characterized by large horizontal dimensions. For example, a typical platform may be 180 m high, its base may have a diameter of 90 to 120 m, and it may have the capacity to store one million barrels of oil.

In more recent times, exploratory drilling is usually carried out with mobile drilling rigs. These include submersible platforms, rendered stationary with chain and wire mooring systems (Barltrop, 1998). They are limited to relatively shallow water, jackup platforms, drill ships or drill barges, and semisubmersible (SS) drilling platforms. The sketches of representative SS platforms are shown in Fig. 1.1 (GBS, jacket, guyed tower, and compliant structures). Such platforms are capable of operating at large depths. The major buoyancy members are placed well below the mean water level under operating conditions to minimize the wave action and to withstand severe weather conditions. They have a relatively low metacentric height (GM) that tends to reduce their pitch and roll motions. With careful design, counteracting inertial forces on surface-piercing columns and on submerged hulls may be made to cancel each other at a certain wave frequency. However, one must be beware of the fact that their high GM limits their variable load. In recent years, their primary station keeping by chain and wire has been augmented by azimuthing thrusters to assist the mooring system and the SS when in transit. The advances in dynamic positioning systems enabled them to operate and to transit at deeper waters without mooring.

What may be called a cousin of SS's is the tension leg platform (TLP). They are similar to SSs in a number of ways. TLPs have a greater water plane area, typically three to six surface-piercing columns, taut vertical mooring tethers, and a complete set of pontoons. All this is made possible because they are stationary.

Spar platforms (Halkyard, 1996) are essentially vertical, almost submerged, circular cylinders kept on station by lateral catenary anchor lines. Their center of gravity is below the center of buoyancy because of the fixed ballast concentrated at their bottom. This gives rise to a relatively large GM, i.e., enhances stability. However, as Barltrop (1998) noted, even though the large draft of a spar significantly reduces heave, its vertical length gives rise to a number of ocean–structure interaction problems: overturning moments that are due to wind, offloading forces, and current-induced forces. The spars are often fitted with spiral strakes to suppress vortex-induced vibrations. If

the effect of the strakes is not experimentally optimized, they may give rise to massive separation at sufficiently high Reynolds numbers and enhance fluid loading and instability.

It should be noted in passing that the center of gravity of a spar may be lowered further (relative to that of a circular cylinder), and giving it a conical shape may further reduce the wave- and current-induced forces: round or hemispherical at the bottom and narrowing toward the free surface (resembling a pear). Above the free surface it may be reduced to a cylinder of constant radius. Such a “pear”-shaped spar has never been used.

The sequence of calculation procedures needed to establish the structural loading generally involves (a) establishing the wave climate in the vicinity of a structure, either on the basis of recorded wave data or by hindcasting from available meteorological data; (b) estimating design wave conditions for the structure; (c) selecting and applying a wave theory to determine the corresponding fluid particle kinematics; (d) using a wave-force formulation to determine the hydrodynamic forces on the structure (often very difficult near the mean water level where wave motion, currents, and strong gusts cannot be quantified); (e) calculating the structural response; and (f) calculating the structural loading, which includes base shear and moment, stresses, and bending moments. These steps may serve only as a rough indicator. The most important fact is that the design of a structure is based on computational fluid dynamics and virtual modeling, as pointed out earlier.

2

Review of the Fundamental Equations and Concepts

2.1 Equations of motion

The equations for an incompressible Newtonian fluid (known as the Navier–Stokes equations) may be written as

$$\frac{\partial u}{\partial t} + u \frac{\partial u}{\partial x} + v \frac{\partial u}{\partial y} + w \frac{\partial u}{\partial z} = X - \frac{1}{\rho} \frac{\partial p}{\partial x} + \nu \left(\frac{\partial^2 u}{\partial x^2} + \frac{\partial^2 u}{\partial y^2} + \frac{\partial^2 u}{\partial z^2} \right) \quad (2.1.1a)$$

$$\frac{\partial v}{\partial t} + u \frac{\partial v}{\partial x} + v \frac{\partial v}{\partial y} + w \frac{\partial v}{\partial z} = Y - \frac{1}{\rho} \frac{\partial p}{\partial y} + \nu \left(\frac{\partial^2 v}{\partial x^2} + \frac{\partial^2 v}{\partial y^2} + \frac{\partial^2 v}{\partial z^2} \right) \quad (2.1.1b)$$

$$\frac{\partial w}{\partial t} + u \frac{\partial w}{\partial x} + v \frac{\partial w}{\partial y} + w \frac{\partial w}{\partial z} = Z - \frac{1}{\rho} \frac{\partial p}{\partial z} + \nu \left(\frac{\partial^2 w}{\partial x^2} + \frac{\partial^2 w}{\partial y^2} + \frac{\partial^2 w}{\partial z^2} \right) \quad (2.1.1c)$$

The equation of continuity is expressed as

$$\frac{\partial u}{\partial x} + \frac{\partial v}{\partial y} + \frac{\partial w}{\partial z} = \text{div } \mathbf{q} = 0 \quad (2.1.2)$$

in which u , v , w represent the velocity components in the x , y , z directions, respectively; X , Y , Z , are the components of the body force per unit mass in the corresponding directions; p is the pressure; and ν is the kinematic viscosity of the fluid. The terms like Du/Dt denote the substantive acceleration. They are also known as the Eulerian derivative, material derivative, or comoving derivative of velocity.

The substantive acceleration consists of a local acceleration (in unsteady flow) that is due to the change of velocity at a given point with time and a convective acceleration that is due to translation, as, for example, in steady flow in a diverging (converging) pipe. The operator D/Dt may be applied to density, temperature, etc., to determine its respective Eulerian derivatives. Obviously, the difference between the substantive acceleration and the local

acceleration in a given direction accounts for the nonlinear convective accelerations, which do not vanish in *nonparallel* flows. In some cases (very slow or creeping motions) the convective accelerations may be neglected. The resulting linear equations are more amenable to analytical and numerical solutions whose upper limit of validity can be determined by experiments and, to some extent, by direct numerical simulations.

The Navier–Stokes equations evolved over a period of 18 years starting with Navier (1827), undergoing different derivations by Poisson (1831), and de Saint Venant (1843), and culminating with Stokes in 1845. However, the boundary conditions (no slip, no penetration) were not established unambiguously. It took another 6 years to firmly set the *hypothesis* that there is no slip on a boundary or, more precisely, the fluid immediately adjacent to the boundary acquires the velocity of the boundary. This was a monumental achievement, *based mostly on heuristic reasoning*, as noted by Stokes (1851): “I shall assume, therefore, as the conditions to be satisfied at the boundaries of the fluid, that the velocity of a fluid particle shall be the same, both in magnitude and direction, as that of the solid particle with which it is in contact.” The derivation of the Navier–Stokes equations for an incompressible Newtonian fluid with constant viscosity may be found in many basic reference texts (see, e.g., Schlichting 1968, or later issues) and is not repeated here.

When gravity is the only body force exerted, a body-force potential may be defined such that $\Omega = -gh$ and

$$X = \frac{\partial \Omega}{\partial x}, \quad Y = \frac{\partial \Omega}{\partial y}, \quad Z = \frac{\partial \Omega}{\partial z}$$

where h is height above a horizontal datum. Then Eqs. (2.1.1) reduce to

$$\frac{Du}{Dt} = -\frac{1}{\rho} \frac{\partial(p + \rho gh)}{\partial x} + \nu \nabla^2 u \quad (2.1.3a)$$

$$\frac{Dv}{Dt} = -\frac{1}{\rho} \frac{\partial(p + \rho gh)}{\partial y} + \nu \nabla^2 v \quad (2.1.3b)$$

$$\frac{Dw}{Dt} = -\frac{1}{\rho} \frac{\partial(p + \rho gh)}{\partial z} + \nu \nabla^2 w \quad (2.1.3c)$$

or, in more convenient vector notation, we have

$$\frac{\partial \mathbf{q}}{\partial t} + (\mathbf{q} \text{ grad})\mathbf{q} = -\frac{1}{\rho} \nabla(p + \rho gh) + \nu \nabla^2 \mathbf{q} \quad (2.1.4)$$

where \mathbf{q} is the velocity vector and may be written as $\mathbf{q} = iu + jv + kw$.

If L is a characteristic length scale and U is a reference velocity, then (2.1.1) can be expressed in dimensionless form by resorting to L and U . Then

it is seen that the ratio UL/v , which is a Reynolds number, represents the ratio of the inertial to viscous forces. In a wide class of flows, the Reynolds number is very large and the viscous terms in the preceding equations are much smaller than the remaining inertial terms over most of the flow field. A notable exception is the *boundary layer* (a brilliant concept discovered by Prandtl 1904) in which the velocity gradients are steep and the viscous stresses are significant.

Through the use of an order-of-magnitude analysis, Prandtl has shown that, for large Reynolds numbers ($Re = U/v$, where x is the distance along the boundary), the equations of motion and continuity for a two-dimensional (2D) flow may be reduced to

$$\frac{\partial u}{\partial t} + u \frac{\partial u}{\partial x} + v \frac{\partial u}{\partial y} = -\frac{1}{\rho} \frac{\partial p}{\partial y} + \nu \frac{\partial^2 u}{\partial y^2} \quad (2.1.5)$$

$$\frac{\partial u}{\partial x} + \frac{\partial v}{\partial y} = 0 \quad (2.1.6)$$

A thorough discussion of all types of steady and unsteady boundary layers is given in Schlichting (1979). As noted earlier, the boundary conditions to be satisfied on the surface of a rigid body are that there will be *no slip* and *no penetration*. The boundary conditions at a free surface are discussed following the introduction of the velocity potential.

2.2 Rotational and irrotational flows

The rates of rotation of a fluid particle about the x , y , and z axes are given by (see, e.g., Schlichting 1968b)

$$\omega_x = \frac{1}{2} \left(\frac{\partial w}{\partial y} - \frac{\partial v}{\partial z} \right), \quad \omega_y = \frac{1}{2} \left(\frac{\partial u}{\partial z} - \frac{\partial w}{\partial x} \right), \quad \omega_z = \frac{1}{2} \left(\frac{\partial v}{\partial x} - \frac{\partial u}{\partial y} \right) \quad (2.2.1)$$

They are components of the rotation vector $\omega = 1/2 \text{ curl } \mathbf{q}$. The flows for which $\text{curl } \mathbf{q} \neq 0$ are said to be rotational because each fluid particle undergoes a rotation as specified by Eq. (2.2.1), in addition to translations and pure straining motions. The absence of rotation, i.e., $\omega_x = \omega_y = \omega_z = 0$, does not, however, require that the fluid be inviscid. In other words, in the regions of flow where $\text{curl } \mathbf{q} = 0$, a real fluid exhibits an irrotational or inviscid-fluid-like behavior because the shear stresses vanish.

Rotation is related to two other fundamental concepts, namely, circulation and vorticity. The circulation Γ is defined as the line integral of the velocity vector taken around a closed curve, enclosing a surface S within the

region of fluid considered. Thus we have

$$\Gamma = \oint \mathbf{q} \cdot d\mathbf{s} = \oint (u dx + v dy + w dz) \quad (2.2.2)$$

According to the Stokes theorem,

$$\Gamma = \oint \mathbf{q} \cdot d\mathbf{s} = \int_S \text{curl } \mathbf{q} \cdot d\mathbf{S} = 2 \int_S \boldsymbol{\omega} \cdot n dS \quad (2.2.3)$$

and therefore (2.2.2) may be written as

$$\Gamma = \iint 2\omega_x dy dz + \iint 2\omega_y dx dz + \iint 2\omega_z dx dy \quad (2.2.4)$$

in which the components of rotation vector appear twice. They are said to be the components of the vorticity vector $\boldsymbol{\zeta}$ such that $\{\zeta_x = 2\omega_x, \zeta_y = 2\omega_y, \zeta_z = 2\omega_z\}$. Thus it follows from (2.2.4) that $\Delta\Gamma = \zeta_n \Delta S$, where ζ_n is the component of the vorticity vector normal to the surface element ΔS . In other words, *the flux of vorticity through the surface is equal to the circulation along the curve enclosing the surface.*

For reference purposes only, we note that in a **frictionless fluid** an element *cannot acquire or lose rotation* (there are no shear forces to induce such a motion); a vortex tube always consists of the same fluid particles, regardless of its motion; and the circulation remains constant with time. These are the fundamental theorems of vorticity and were enunciated by Helmholtz (1858) and Lord Kelvin (see Sir William Thomson 1849). For a detailed discussion of these theorems the reader is referred to classic reference texts such as Batchelor (1967), Milne-Thomson (1960), or Lamb (1932).

In *real fluids*, vorticity may be generated, redistributed, diffused, and destroyed because the frictional forces are not conservative. In other words, vorticity is ultimately dissipated by viscosity to which it owes its creation. For example, the vorticity found in a vortex about four diameters downstream from a circular cylinder is about 70% of the vorticity shed from the separation point (Bloor and Gerrard 1966). Schmidt and Tilmann (1972) found a 50% reduction in circulation as the vortices move from 5-diameter to 12-diameter downstream positions. The remainder is partly diffused and partly canceled by the ingestion of fluid bearing oppositely signed vorticity. One should also bear in mind that the experiments yield only the *normal component* of vorticity. Thus the consequences of the stretching and twisting of vortex filaments as a consequence of three dimensionality in the wake of a body and hence the redistribution of vorticity into directions other than the normal are not accounted for. This relatively simple example points out not only some of the difficulties associated with the use of the inviscid-fluid